# Structural and Kinetic Studies of the Y73E Mutant of Octaheme Cytochrome $c_3$ ($M_r$ = 26 000) from *Desulfovibrio desulfuricans* Norway[‡]

Corinne Aubert,[§] Marie-Thérèse Giudici-Orticoni,[§] Mirjam Czjzek,*[,||] Richard Haser,[||] Mireille Bruschi,[§] and Alain Dolla[§]

*Unité de Bioénergétique et Ingénierie de Protéines, UPR 9036, CNRS, and Unité de Architecture et Fonction des Macromolécules Biologiques, UPR 9039, CNRS, Institut de Biologie Structurale et Microbiologie, 31 chemin Joseph-Aiguier, 13402 Marseille Cedex 20, France*

*Received July 9, 1997; Revised Manuscript Received October 31, 1997*

ABSTRACT: A combination of structural, kinetic, and interaction experiments has been used to study the role of a highly conserved aromatic residue, Tyr73, parallel to the sixth heme axial ligand of heme 4 in multiheme cytochrome $c_3$ ($M_r$ = 26 000), also called cytochrome $cc_3$ or octaheme cytochrome, from *Desulfovibrio desulfuricans* Norway. This residue is expected to be involved in intermolecular electron transfer and protein−protein interaction, since heme 4 is described to be the interaction site between physiological partners. The kinetic experiments show that the Y73E replacement provokes no significant change in the electron-transfer reaction with the physiological partner, the [NiFeSe] hydrogenase, but that the protein−protein interaction between cytochrome $c_3$ ($M_r$ = 26 000) and hydrogenase is strongly affected by the mutation. The aromatic residue does not play a role in maintaining the axial heme ligand in a particular orientation, since the mutation did not affect the orientation of histidine 77, the sixth axial ligand of heme 4. The structural analysis by X-ray crystallography clearly shows that a rearrangement of the charged residues in the vicinity of the mutation site is responsible for the change in protein−protein interaction, which is of an electrostatic nature. Lys22 and Arg66, residues which are located at the interacting surface, are twisted toward the mutated position Glu73 in order to compensate for the negative charge and therefore are no longer accessible for the docking with a physiological partner. Tyr73 has instead a structural function and probably a role in maintaining the hydrophobic environment of the heme 4 cavity rather than a function in the intermolecular electron transfer with the physiological partners.

The relationship between amino acid sequence, folding, and protein function is not yet well understood and is matter of current research. One possible way to investigate this relationship is the analysis of the effect of a single replacement on the functional properties of the protein in question. *c*-type cytochromes have been extensively studied in order to elucidate the structural and functional basis of electron transfer mediated by this type of redox protein (*1*−*3*). In particular, the roles of several invariantly conserved amino acid residues in cytochrome *c* have been specified by means of protein engineering (*4*). While numerous experiments have been performed on monoheme cytochromes *c*, the analysis of multiheme *c*-type cytochromes by mutagenesis is not yet extensively used.

Several types of soluble polyheme cytochromes *c* have been isolated and characterized in the anaerobic, sulfate-reducing bacteria belonging to the genus *Desulfovibrio*. These include the tetraheme cytochrome $c_3$ ($M_r$ = 13 000) (*5*), the octaheme cytochrome $c_3$ ($M_r$ = 26 000) (*6*), and the hexadecaheme cytochrome Hmc (*7*). All these cytochromes belong to the class III described by Ambler (*8*). Three-dimensional structures of various tetraheme cytochromes $c_3$ are available (ref *9* and references therein), as well as that of the octaheme cytochrome $c_3$ (*10*). They have been grouped together in a superfamily, in which the basic unit would be the tetraheme cytochrome $c_3$ ($M_r$ = 13 000) type (*6*). Their particularity is the presence of several heme groups of extremely negative oxidoreduction potentials, ranging from −400 to −165 mV (*11*) compared to about 270 mV exhibited by the mitochondrial-type monoheme cytochrome *c* (*12*). The negative redox potential values are correlated with the involvement of these polyheme cytochromes in the reduction of poor oxidants in the anaerobic sulfate-reduction pathways.

In the past few years, the development of genetic studies of the sulfate-reducing bacteria has led to the identification of the genes encoding these multiheme cytochromes (*7*, *13*, *14*) and therefore making the use of site-directed mutagenesis accessible for analysis of these proteins. Protein engineering has already been used for the tetraheme cytochrome $c_3$, to study the influence of the histidine, the sixth axial ligand to the heme iron atom, which has been replaced by a methionine residue (*15*). This study has emphasized the role of the sixth axial ligand in the modulation of the redox potential of the heme groups. These site specific replacements have also allowed us to identify heme 4 (sequential numbering) in the cytochrome $c_3$ as the heme involved in the intermolecular

[‡] Atomic coordinates for the mutant structure have been deposited with the Brookhaven Protein Data Bank as entry 1AQE.

* To whom correspondence should be sent. Telephone: 04 91 16 45 13. Fax: 04 91 16 45 36. E-mail: czjzek@afmb.cnrs-mrs.fr.

[§] Unité de Bioénergétique et Ingénierie de Protéines.

[||] Unité de Architecture et Fonction des Macromolécules Biologiques.

S0006-2960(97)01656-5 CCC: $15.00 
Published on Web 02/06/1998

electron-transfer reaction with its physiological partner, the hydrogenase (*15*). Recently, the site-directed mutagenesis study of a strictly conserved aromatic residue throughout the entire cytochrome $c_3$ family has been reported (*16*). The study indicates that the replacement of that residue, namely Phe20, by an isoleucine or a tyrosine in the DvH tetraheme cytochrome $c_3$ has only small effects on the redox potential of the heme groups. Moreover, it appears that this aromatic residue has no essential role in either electron−electron or electron−proton cooperativity (*16*).

Among the conserved aromatic residues, tyrosine 73 in octaheme cytochrome $c_3$ is an interesting candidate, since it is present in all the different cytochromes $c_3$ except one, the tetraheme cytochrome $c_3$ from the same bacterial strain *Desulfovibrio desulfuricans* Norway, where it is replaced by a glutamate (*17, 18*). Tyrosine 66 of cytochromes $c_3$ from DvH,[1] DvM, Dg, and Dd is structurally superimposable on Y73 in the octaheme cytochrome (*10*). The side chain of this tyrosine is parallel to the imidazole ring of histidine 77 (70 in DvH, DvM, Dg, and Dd), the sixth axial ligand of heme 4. The observation that, for three of the four hemes there always is an aromatic residue parallel to one of the histidine axial ligands, has already led to the supposition of an important functional role of these aromatic residues (*18, 19*). Furthermore, this residue is located on the same side as the solvent-exposed edge of heme 4 (*10*) and therefore is possibly implicated in the region of protein−protein interaction on complex formation with physiological partners. It has been proposed that the [NiFeSe] hydrogenase is the physiological partner of the octaheme cytochrome $c_3$ in the electron-transport chain involved in sulfate respiration (*20, 21*). Preliminary results with the Y73E substitution in octaheme cytochrome $c_3$ from *D. desulfuricans* Norway showed that this replacement strongly affected the interaction process between the hydrogenase and the cytochrome (*14*). We report here the analysis of this Y73E mutant with respect to the structural and functional effects of this point mutation. To specify the role of this aromatic residue in the electron-transfer reaction, we have performed accurate determinations of the thermodynamic parameters of the complex formation with hydrogenase and of the intermolecular kinetic constants. The kinetic results are discussed on the basis of the three-dimensional structure of the Y73E mutant octaheme cytochrome $c_3$, which has been established at 2.2 Å resolution.

## EXPERIMENTAL PROCEDURES

*Purification of Periplasmic [NiFeSe] Hydrogenase from Desulfovibrio desulfuricans Norway*. Approximately 200 g of wet weight cells from DdN from 300 L fermentations in Starkey's medium (*22*) was harvested at the exponential phase ($OD_{600} = 0.6$). Cells were resuspended in 400 mL of 50 mM Tris hydrochloride/50 mM EDTA buffer (pH 9) supplemented with various protease inhibitors (100 $\mu$M leupeptin, 1 $\mu$M pepstatin A, and 500 $\mu$M PMSF). During the purification procedure, the hydrogenase activity was measured as described below.

The mixture was stirred for 30 min at 37 °C and centrifuged for 1 h at 6500*g*. The supernatant, containing the periplasmic proteins, was adjusted to pH 7.6 and dialyzed overnight against 20 mM Tris hydrochloride (pH 7.6), 20 mM NaCl, and 5 mM EDTA. All purification steps were performed at 4 °C. All buffers were preincubated under argon to remove any oxygen traces and adjusted to pH 7.6. The periplasmic fraction was centrifuged for 1 h at 6500*g* and absorbed onto a DEAE-cellulose column (Whatman DE52), equilibrated with 20 mM Tris hydrochloride, 20 mM NaCl, and 5 mM EDTA buffer. The column was washed with approximately 2 column volumes of buffer and was eluted with a gradient of 20 mM Tris hydrochloride, 20 mM NaCl, and 5 mM EDTA to 20 mM Tris hydrochloride, 500 mM NaCl, and 5 mM EDTA. The hydrogenase fraction that eluted at 400 mM NaCl was then loaded onto a hydroxyapatite column, equilibrated with the same buffer. The fraction with hydrogenase activity was eluted with 100 mM phosphate buffer and dialyzed overnight against 20 mM Tris hydrochloride buffer. The subsequent chromatography step was carried out on a FPLC apparatus. The dialyzed fraction was loaded onto a Mono-Q column (Pharmacia Fine Chemicals), equilibrated with 20 mM Tris hydrochloride. The protein was eluted with a gradient of 20 mM Tris hydrochloride and 20 mM NaCl to 500 mM Tris hydrochloride and 500 mM NaCl.

The [NiFeSe] hydrogenase obtained after elution with 85 mM Tris hydrochloride and 85 mM NaCl has a purity index [$A_{390ox}/A_{280ox}$] of 0.305 and was found to be pure by native and sodium dodecyl sulfate−polyacrylamide gel electrophoresis using a PhastSystem apparatus (Pharmacia) as well as by protein sequencing. The diluted fraction was concentrated and dialyzed by ultrafiltration through an Amicon centricon 30 membrane concentrator. Forty-five milligrams of pure hydrogenase with a specific activity of 46 units/mg in a hydrogen consumption assay was obtained from 200 g of bacteria.

*Determination of the Hydrogenase Activity.* The hydrogenase activity was measured using the following procedure. Anaerobic cuvettes of 1 mL containing 1 mM MEV, 50 mM Hepes (pH 7.6), 25 mM glucose, 0.5 unit of glucose oxidase, and 250 units of catalase were subjected to three alternating cycles of argon and hydrogen flushes. The cuvettes remained under an overpressure of 20 kPa of hydrogen after the final cycle, and the $H_2$ concentration was approximately 200 mM. The hydrogenase was preincubated with hydrogen, and the absorbance was measured at 604 nm after the addition of the enzyme, using a single-beam Beckman DU 7500 spectrophotometer. The slope of the tangent drawn at the start of the record was used to calculate the hydrogen oxidation rate with an absorption coefficient of 13 600 $M^{-1}$ $cm^{-1}$ for methyl viologen.

*Purification of Cytochromes.* Wild-type and mutant DdN octaheme cytochromes $c_3$ were prepared by the methods described elsewhere (*14*). The cytochrome concentrations were determined spectrophotometrically using an absorption

[1] Abbreviations: DdN, *Desulfovibrio desulfuricans* Norway; DvH, *Desulfovibrio vulgaris* Hildenborough; DvM, *Desulfovibrio vulgaris* Miyazaki; Dg, *Desulfovibrio gigas*; Dd, *Desulfovibrio desulfuricans* ATCC 27774; rmsd, root-mean-square deviation; EDTA, (ethylenedinitrilo)tetraacetic acid; PMSF, phenylmethanesulfonyl fluoride; MEV, methyl viologen; EDC, *N*-ethyl-*N*′-[3-(dimethylamino)propyl]carbodiimide hydrochloride; NHS, *N*-hydroxysuccinimide; MES, 4-morpholineethanesulfonic acid; Hepes, *N*-(2-hydroxyethyl)piperazine-*N*′-2-ethanesulfonic acid; RU, resonance unit; octaheme cytochrome $c_3$, cytochrome $c_3$ ($M_r = 26\,000$), also called cytochrome $cc_3$ or octaheme cytochrome.

Table 1: Data Collection and Refinement Parameters for Y73E Octaheme Cytochrome $c_3$

| | |
|---|---|
| space group | $P3_121$ |
| cell dimensions (Å) | $a = b = 72.62$ and $c = 60.32$ |
| resolution range (Å) | 22.0−2.16 |
| total no. of observations | 53789 |
| no. of unique observations | 9870 |
| % of data/$R_{sym}$ | 97.0/9.6 |
| no. of non-hydrogen atoms | 1031 |
| no. of solvent sites | 102 |
| ions modeled | $1SO_4^{2-}$ |
| missing residues | Glu1 |
| $R$-factor (%)/no. of reflections | 17.9 (1$\sigma$ cutoff)/8992 |
| $R_{free}$ (%)/no. of reflections | 23.9 (1$\sigma$ cutoff)/944 |
| rms deviations | |
| bond lengths (Å) | 0.008 |
| bond angles (deg) | 1.82 |
| Ramachandran outliers | none |

coefficient $\epsilon$ of 245 200 $M^{-1}$ $cm^{-1}$ at 553 nm in the reduced state.

*Biosensor Analysis*. The interaction between [NiFeSe] hydrogenase and both wild-type and mutant cytochromes was investigated with a biomolecular interaction analysis biosensor-based analytical system (BIAcore; Pharmacia). All experiments were performed at 25 °C. The hydrogenase dissolved in 10 mM MES (pH 5) and was immobilized on a CM5 sensor chip (Pharmacia biosensor) through amine coupling. The carboxylic acid groups of a dextran matrix were activated with 70 $\mu$L (10 $\mu$L/min) of a mixture of 0.2 M EDC and 0.05 M NHS. The enzyme was injected over the course of 7 min (10 $\mu$L/min), resulting in approximately 3000 resonance units of immobilized protein, and the reaction was stopped by the injection of 70 $\mu$L (10 $\mu$L/min) of 1 M ethanolamine hydrochloride in order to transform the remaining active esters into amides. This unit is used to express the surface plasmonic resonance signal. One thousand resonance units is equivalent to a change of about 1 mg/mm$^2$ in surface protein concentration (Biosensor AB). This procedure allows the hydrogenase to be covalently coupled to the carboxymethyl dextran-modified gold surface via the exposed amino groups. Both cytochromes were diluted in 50 mM Hepes buffers at either pH 7.6, 5, or 8.5 and injected using a constant flow rate of 30 $\mu$L/min (100 $\mu$L). The resulting sensorgrams were evaluated using the biomolecular interaction analysis evaluation software (BIAcore) in order to calculate the kinetic constants of the complex formation.

*Kinetic Experiments*. The kinetic assays were performed using anaerobic cuvettes. The cuvettes were filled with different concentrations of wild-type and mutant cytochromes, 50 mM Hepes (pH 7.6), 25 mM glucose, 0.5 unit/mL glucose oxidase, and 250 units/mL catalase. The hydrogenase and the cuvettes were made anaerobic as previously described in the activity experiments. The cytochrome reduction rate was determined on the basis of the absorption band at 553 nm and by using the slope of the tangent drawn at the beginning of the recording.

The equations generated by kinetic models were fitted to the data using the Marquardt algorithm (*23*). The $k_{cat}$ and $K_m$ of both cytochromes were determined by nonlinear least-squares fitting of the Michaelis−Menten equation to the data.

*X-ray Structure Determination.* Crystals of the Y73E mutant were grown under conditions similar to those of the wild-type protein (*24*). Hanging drop vapor diffusion was employed with $(NH_4)_2SO_4$ as the precipitating agent (1.4−1.6 M solution). Crystals of the mutant grew isomorphously to those of the wild type and are of the space group $P3_121$. Unit cell dimensions are summarized in Table 1.

The Y73E mutant data set was collected up to 2.16 Å resolution from a single crystal on a diffractometer equipped with a Rigaku R600 rotating anode, operated at 40 mA and 80 kV, and an MAR imaging plate bidimensional detector. The intensity integration and data treatment were performed with the DENZO program package (*25*, *26*). Since the unit cell parameters changed by more than 1 Å, the correct orientation of the protein molecule within the new unit cell was found by molecular replacement using the program AMoRe (*27*). A single solution with a correlation coefficient of 57.5% and an $R$-factor of 36.3% was obtained. The structural refinement was carried out with the XPLOR3.8 program package (*28*). Bulk solvent was modeled in order to include all data from very low resolution up to the highest

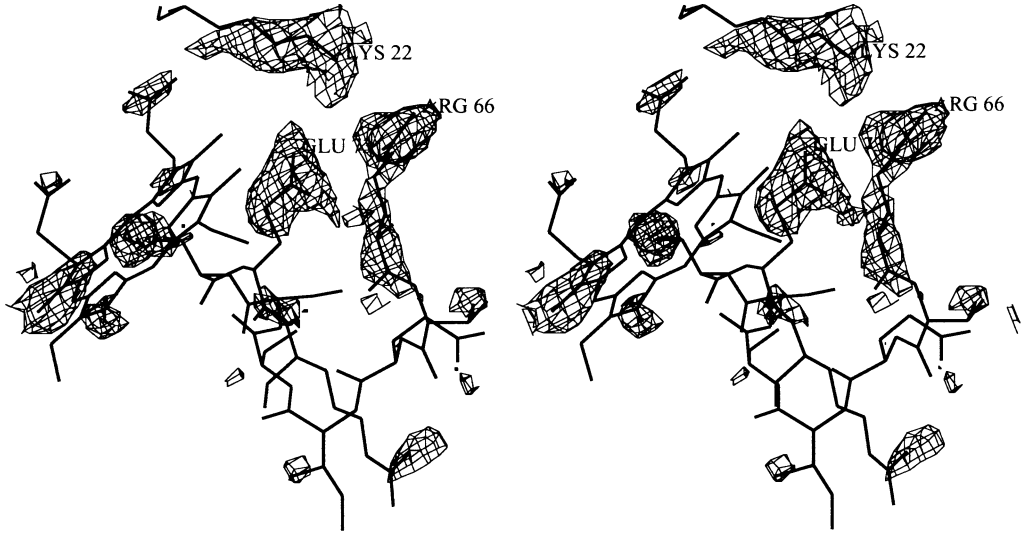


FIGURE 1: Stereodrawing of the difference electron density map in the immediate vicinity of the mutated residue. This $F_o - F_c$ map was calculated after a first X-PLOR refinement cycle with the wild-type model. Only positive electron density at a 3$\sigma$ level is shown. Overlaid is the final refined mutant protein structure obtained. The figure was produced with TURBO-FRODO (*38*).

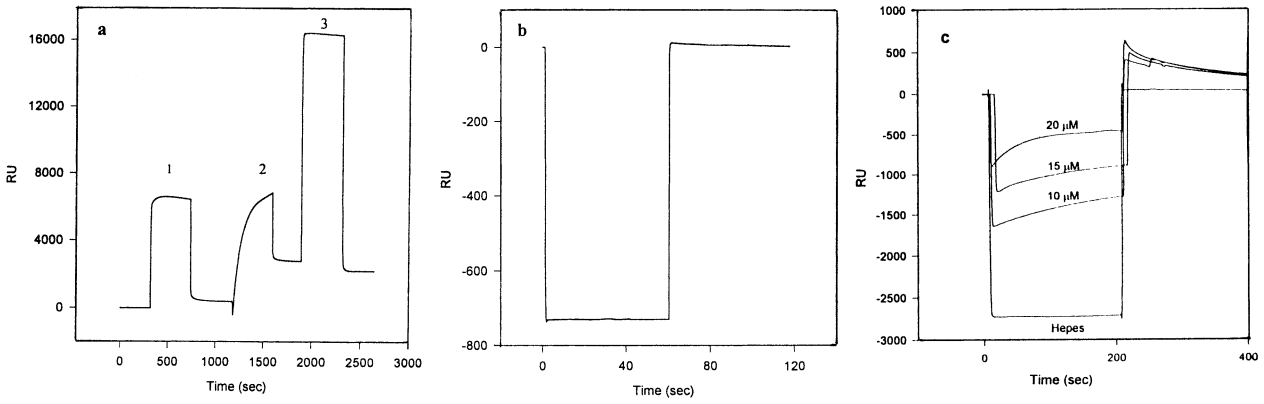


FIGURE 2: (a) Sensorgram from immobilization of [NiFeSe] hydrogenase using amine coupling: (1) activation of the dextran by an NHS/EDC mixture, (2) injection of 110 $\mu$g/mL hydrogenase, and (3) deactivation of unreacted NHS esters using ethanolamine hydrochloride at pH 8.5. (b) Control experiment. No protein was immobilized, with injection of 15 $\mu$M wild-type cytochrome diluted in 50 mM Hepes at pH 7.0. (c) Sensorgrams showing the interaction between hydrogenase and increasing concentrations (10, 15, and 20 $\mu$M) of wild-type cytochrome.

resolution. The initial difference electron density map is shown in the vicinity of the mutation site in Figure 1. This initial $F_o - F_c$ map allowed us to model the alterations due to the mutation. $F_o - F_c$ and $3F_o - 2F_c$ maps were calculated and inspected after each XPLOR slow cooling procedure in order to adjust side chain alterations and to check the water molecules. The final model included 110 out of 111 residues; the N-terminal residue, for which no density was observed, could not be modeled. Besides the four heme groups, the model also included a sulfate anion and 102 water molecules, modeled as single oxygen atoms. The final refinement parameters are summarized in Table 1. The structure exhibits good stereochemistry as has been verified with the program PROCHECK (*29*), and the estimated coordinate errors are about 0.20 Å (*30*). The heme numbering scheme, adopted in this structure description, corresponds to the order of appearance in the primary sequence of the cysteines that covalently link the heme groups.

*Dipole Moment Calculation*. The dipole moment together with the electrostatic calculation and analysis was calculated using the GRASP software (*31*) running on a Silicon Graphics workstation. The potential maps were calculated with a Poisson−Boltzmann solver (*32*), on the basis of a CHARMM-derived parameter file.

## RESULTS

*Interaction between both Wild-Type and Y73E Octaheme Cytochromes $c_3$ and [NiFeSe] Hydrogenase from Desulfovibrio desulfuricans Norway*. Amine coupling was based on favorable electrostatic attraction between negative charges of the dextran carboxylic groups and positive charges on the immobilized ligand. Either cytochrome or hydrogenase can be covalently coupled to the CM5 sensor chip. However, cytochrome immobilization was discarded since the lysine and arginine residues located around the heme 4 crevice are supposed to be the site of interaction with the redox partners. Therefore, we chose to covalently immobilize hydrogenase (p$I$ = 6) on the biosensor. The immobilization of the enzyme was preliminarily performed by testing the appropriate pH buffer for the covalent binding with the carboxymethyl dextran. To select the optimal conditions for electrostatic interactions, three buffers with different pHs were used: 10 mM acetate at pH 4, 10 mM MES at pH 5, and 10 mM Hepes at pH 7. Covalent binding in 10 mM MES buffer (pH 5) showed both a good specificity and a progressive attachment as illustrated in Figure 2a. To study the hydrogenase stability, the enzyme was preincubated in either 10 mM MES at pH 5 or 10 mM Hepes at pH 7 for up to 90 min and the activity at pH 7 was measured as described in Experimental Procedures. No differences were found between pH 5 and 7. Injection of 70 $\mu$L of hydrogenase (100 $\mu$g/mL, 10 mM MES at pH 5) corresponded to approximately 3000 RU.

Wild-type and Y73E cytochromes were diluted in either 10 mM Hepes at pH 7 or 10 mM glycylglycine buffer at pH 8.5 and injected on either activated or nonactivated dextran (Figure 2b). No binding was detected, which is in total agreement with the acidic property of these cytochromes. In all experiments, the hydrogenase and the cytochromes were in an oxidized state.

The interaction of immobilized hydrogenase with three different amounts (10, 15, and 20 $\mu$mol) of wild-type octaheme cytochrome $c_3$ at pH 7.6 is illustrated in Figure 2c. The sensorgrams reflect the association and dissociation of the two proteins and are proportional to the protein amount. The strong decrease of the resonance unit number at the injection time was only due to the buffer effect (Figure 2c). The association rate constant, $k_{on}$, and the dissociation rate constant, $k_{off}$, were determined for each cytochrome concentration and are indicated in Table 2.

These values were consistent with the three tests described by Schuck and Minton (*33*) for the kinetic analysis of biosensor data. The apparent equilibrium dissociation constant was deduced from the ratio of the two kinetic constants ($k_{off}/k_{on}$). Measurements at three different cytochrome concentrations allowed us to obtain an average value for the apparent equilibrium dissociation constant of $3.6 \times 10^{-6}$ M.

On the other hand, when mutant cytochrome is used in the same experiment, no binding was observed, even for cytochrome concentrations of up to 550 $\mu$M. Since the experimental limit of our measurement is situated around $10^{-3}-10^{-4}$ M, the value of the apparent equilibrium dissociation constant for the mutant protein should be higher than this.

Table 2: Association and Dissociation Constants[a] for the Binding of Wild-Type and Y73E Octaheme Cytochromes $c_3$ to Immobilized Hydrogenase

| cytochrome ($\mu$M) | $k_{on}$ ($M^{-1}$ $s^{-1}$) | $k_{off}$ ($s^{-1}$) | $K_d$ (M) |
|---|---|---|---|
| wild-type (20) | $1.2 \times 10^3 \pm 2.83$ | $3.9 \times 10^{-3} \pm 1.8 \times 10^{-5}$ | $3.25 \times 10^{-6}$ |
| wild-type (15) | $1.9 \times 10^3 \pm 56.8$ | $2.8 \times 10^{-3} \pm 3.7 \times 10^{-5}$ | $1.5 \times 10^{-6}$ |
| wild-type (10) | $6.1 \times 10^2 \pm 58.7$ | $3.4 \times 10^{-3} \pm 2.23 \times 10^{-5}$ | $5.5 \times 10^{-6}$ |
| Y73E mutant (550) | ND | ND | $>10^{-3}-10^{-4}$ |

[a] Kinetic constants were determined using BIAlogue Kinetics Evaluation Software. The kinetic data are interpreted on the basis of the simple binding model L + A ↔ LA, where L denotes the mobile ligand and A the immobilized receptor. $k_{off}$ and $k_{on}$ values were obtained from the dissociation and association experiments by directly fitting the equations $R_0 \exp[-k_{off}(t-t_0)]$ to the raw dissociation data and $(k_{on}CR_{max}/k_{on}Cnk_{off})[1 - \exp[(k_{on}Cn+k_{off})(t-t_0)]]$ to the raw association data, respectively (see also Figure 2). The apparent equilibrium dissociation constant $K_d$ was directly calculated from the ratio $k_{off}/k_{on}$. $k_{obs}$ values were obtained by fitting the equation $R(t) = R_{0a} + (R_{\infty a} - R_{0a})[1 - \exp(-k_{obs}t)]$ (*33*) to the raw data for the octaheme cytochrome $c_3$ concentrations. The $k_{on}$ and $k_{off}$ values were determined by linear regression of the $k_{obs}$ values as a function of octaheme cytochrome $c_3$ concentrations.

To test whether the pH has an effect on the interaction between cytochromes and hydrogenase, experiments were performed at pH 5 and 8.5. At pH 5.0, injection of either wild-type or mutant cytochrome above dextran already induced a response. To minimize this effect, soluble carboxymethyl dextran was added to the cytochrome solutions. Under these conditions, no significant difference in the rate constants of association or dissociation of either cytochrome with the hydrogenase was measured, whatever the pH. The protonation state of the glutamate residue does not seem to influence the interaction between the two proteins.

*Electron Transfer between Hydrogenase and both Wild-Type and Mutant Octaheme Cytochrome $c_3$.* The results described above show that substitution of the tyrosine 73 by a glutamate in octaheme cytochrome $c_3$ strongly affected the interaction with the [NiFeSe] hydrogenase. To analyze the effect of this mutation on the electron transfer between the two partners, we studied the kinetics of reduction of either wild-type or mutant cytochromes by the hydrogenase. Reduction of cytochromes by the [NiFeSe] hydrogenase at the steady state was studied spectrophotometrically as described in Experimental Procedures. The hydrogenase was in a reduced state, and the cytochromes were in an oxidized state. Moreover, under our conditions, reduced hydrogenase can be considered constant during the reaction due to the excess of molecular hydrogen. The $K_m(H_2)$ has been determined for the [Fe] hydrogenase from *Clostridium pasteurianum* and was found to be on the order of 30−300 $\mu$M (*34*); therefore, the $H_2$ concentration of about 200 mM can be considered saturating and the hydrogenase recduced. Consequently, the equilibrium is irreversible and totally shifted to the reduction of cytochromes. In these experiments, the hydrogenase concentration was 22 nM and the concentration of the wild-type octaheme cytochrome $c_3$ varied from 0 to 25 $\mu$M. In the experiments with Y73E octaheme cytochrome $c_3$, the concentration varied from 0 to 70 $\mu$M.

Table 3: Kinetics of Electron Transfer between [NiFeSe] Hydrogenase and either Wild-Type or Y73E Mutant Cytochromes[a]

| | $k_{cat}$ ($s^{-1}$) | $K_m$ ($\mu$M) | $k_{cat}/K_m$ ($\mu M^{-1}$ $s^{-1}$) |
|---|---|---|---|
| wild-type | $8.09 \pm 2.15$ | $8.89 \pm 17$ | 0.91 |
| Y73E | $8.63 \pm 1.16$ | $129.5 \pm 24.3$ | 0.066 |

[a] The errors on $K_m$ and $k_{cat}$ values were obtained by the least-squares method.

The steady-state rate of reduction of either wild-type or mutant cytochrome followed Michaelis−Menten kinetics (Figure 3). Fitting the curves to the Michaelis−Menten equation suggests a lack of intermolecular cooperativity between the redox centers. In the same way, Verhagen et al. (*35*) have previously demonstrated that the electron transfer between a monoheme cytochrome $c_{553}$, a tetraheme cytochrome $c_3$, and [Fe] hydrogenase from DvH followed Michaelis−Menten kinetics as well. The Michaelis−Menten constant deduced from our data was found to be 8.9 $\mu$M for the wild-type cytochrome and 130 $\mu$M for the Y73E cytochrome at pH 7 and 25 °C (Table 3). It should be noted that these values, deduced from the Lineweaver−Burke plots, are on the same order of magnitude. The 14-fold difference between $K_m$ values of both cytochromes could be explained by the effect of the mutation on the interaction between the two partners. This result is in total agreement with the BIAcore experiments described above. On the other hand,

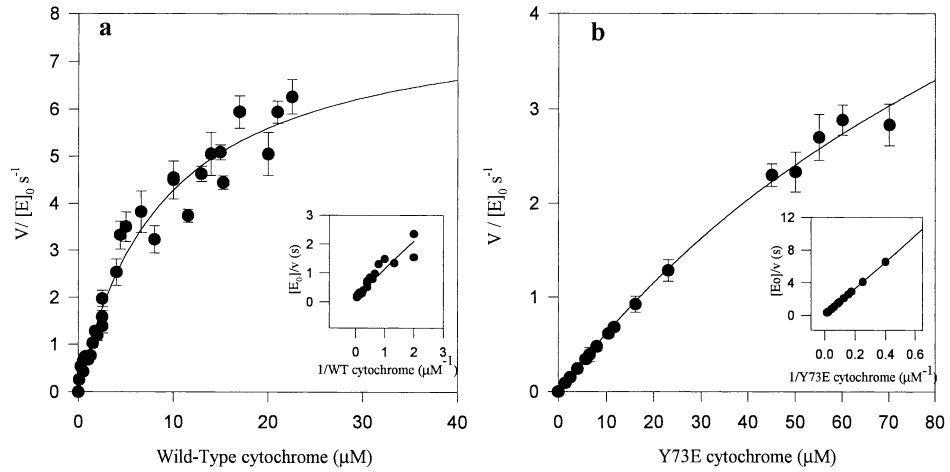


FIGURE 3: (a) Kinetic behavior of the reaction between wild-type octaheme cytochrome $c_3$ and hydrogenase. The reduction of cytochrome was measured in 50 mM Hepes at pH 7.0. (b) Kinetic behavior of the reduction of mutant Y73E cytochrome by hydrogenase. The reduction was measured under the same conditions as in panel a. The inserts show the corresponding Lineweaver−Burke plots.

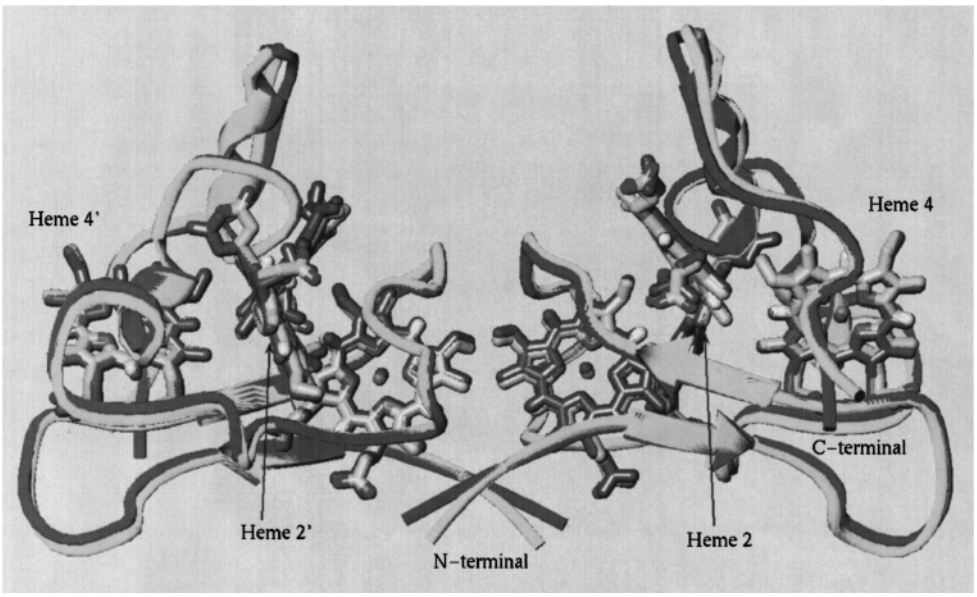


FIGURE 4: Ribbon representation of the dimeric unit. The figure was produced with TURBO-FRODO (*38*). The wild-type protein structure is represented in yellow, while the mutant structure is represented in magenta. The deviations for the loop regions are visible, such as the rather large positional changes of the propionate groups of heme 2.

the $k_{cat}$ value was found to be on the same order of magnitude for wild-type and mutant cytochromes. This implies that the ratio $k_{cat}/K_m$ is about 14-fold higher for the wild-type cytochrome than for the Y73E mutant cytochrome. The results obtained from the kinetic experiments show clearly that the replacement of tyrosine 73 by a glutamate has no impact on steady-state rate of electron transfer but strongly affects the complex formation between the [NiFeSe] hydrogenase and the octaheme cytochrome $c_3$.

The electrophoresis on polyacrylamide gel under denaturing conditions of both oxidized and hydrogenase-reduced cytochromes shows only one band of about 26 000 Da. Therefore, reduction of the dimeric cytochrome by hydrogenase does not induce a dissociation of the subunits. The same result was obtained with the mutant cytochrome (data not shown).

*Three-Dimensional Structure of the Octaheme Y73E Cytochrome $c_3$.* As is evident in Figure 4, the overall structural fold has not been changed drastically by the site specific replacement. The molecular packing is mainly the same in the two crystal structures, however a little less dense in the case of the mutant structure (65% solvent instead of 60% for the wild-type crystals), also reflected by the changes of the unit cell parameters. Different solvent contents for the cytochrome crystals had already been observed for the wild-type protein (*24*); therefore, the observed unit cell parameter variation seems to not be related to the point mutation.

The superposition of mutant and wild-type cytochromes is shown in Figure 4. The overall root-mean-square deviation (rmsd) is rather high, 1.2 Å (0.82 Å for Cα only). The rmsd of 0.59 Å is obtained when the N- (Thr2) and C-terminal (Gln110) residues and residues 18, 19, 18′, and 19′ of loop 1 are excluded from the calculation. All these residues are substantially disordered, even in the wild-type structure (*10*), and the large positional deviations observed are therefore the result of the flexibility of these regions rather than the result of the mutation. In the wild-type protein, the side chain of Tyr73 is almost parallel to the pyrrole plane of His77, the sixth axial ligand of heme 4. Thus, mutation of this residue into a negative charge will change the hydrophobic environment of the heme crevice and possibly influence the redox potential.

The changes introduced by the point mutation can be generally described as a rearrangement of the charged residues in the vicinity of the mutation, since an uncharged residue has been replaced by a negatively charged one. The most striking changes are observed for the side chains of two positivly charged residues, Lys22 and Arg66, which are reoriented toward the newly introduced negative charge (in order to compensate for it) (Figures 5 and 6), and one of the propionate groups of heme 2, which forms a salt bridge with Arg74, formed in a different way in the wild-type crystal structure (Tables 4 and 5). Furthermore, one can observe that almost all charged residues around the solvent-exposed heme edge of heme 4 have undergone a conformational change (Table 4). This is probably only partly due to the mutation, since most of these residues are pointing into the solvent region and therefore are flexible in both structures. But a change in the distribution of the charges caused by the mutation is also expected, since a neutral residue has been replaced by a negatively charged one. The rearrangement of the charge distribution can also be visualized by the vector representation of the dipole moment (yellow arrows in Figure 5a,b). The dipole moment is attenuated in the case of the mutant protein, and it also has slightly changed its orientation. In the wild-type protein, the arrow is almost perfectly perpendicular to the exposed heme edge surface of heme 4, superposable with Cys105, highly exposed to the surface, while in the mutant structure, the dipole moment is no longer perpendicular to this edge but tilted closer to the axial ligand, His109, on the opposite side relative to the mutation.

*Heme Environments.* Important parameters for the modulation of electron transfer are the solvent exposure of the hemes, the axial ligands, and the heme propionate environments (*36*, *37*). The calculated values of solvent-exposed area [TURBO-FRODO software (*38*); $H_2O$ radius of 1.4 Å] obtained for the heme groups and some of the involved

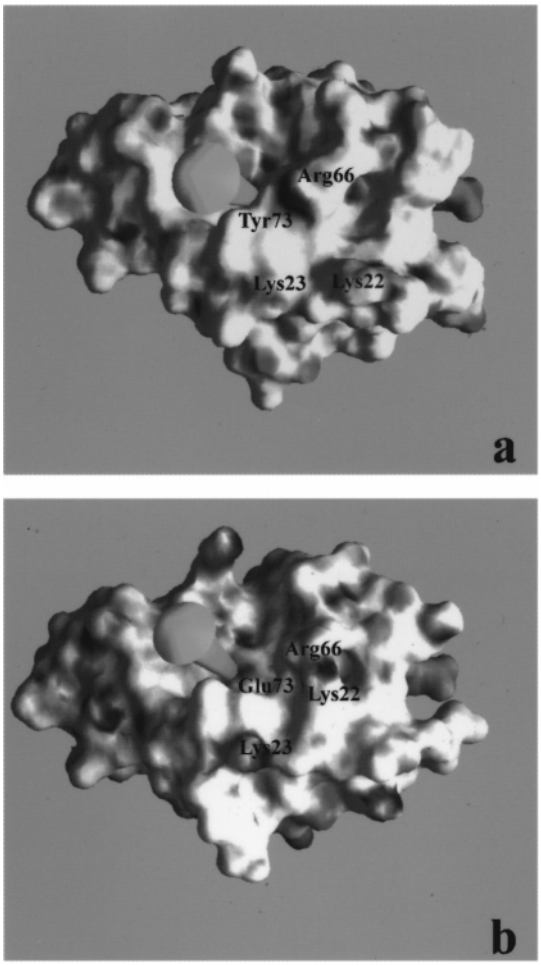


FIGURE 5: (a) Molecular surface representing the charge distribution around the solvent-exposed heme edge of heme 4 for the wild-type octaheme cytochrome $c_3$. (b) The molecular surface for the mutant Y73E cytochrome. The yellow arrows represent the orientation of the respective dipole moments of the molecules as calculated with GRASP (*31*). The relative orientations for both illustrations are essentially the same. The illustrations were produced with GRASP.

histidine and cysteine residues for the wild-type and mutant protein structures are listed in Table 6. Significant changes are observed in the cases of hemes 2 and 4, the heme groups closest to the mutational site (distances to the mutational site, heme 1−Glu73 C$\gamma$ = 20.85 Å, heme 2−Glu73 C$\gamma$ = 14.69 Å, heme 3−Glu73 C$\gamma$ = 17.38 Å, and heme 4−Glu73 C$\gamma$ = 6.61 Å). Interestingly, the heme edge exposure changes much less for heme 4 than for heme 2. In fact, the rearrangement of loop 3 (loop 3, residues 64−68; see also ref *10*) and the conformational change of the side chain of Arg74 account for the marked diminution of the solvent exposure of heme 2, and only Lys22 and Lys23 and the mutation itself concern the solvent exposure of the heme edge of heme 4. The mutation, however, has an impact on the solvent exposure of His77, the sixth axial ligand of heme 4, for which the solvent-exposed region has doubled. The value now compares well to the corresponding histidine in the tetraheme cytochrome $c_3$ from DdN, where a glutamate is actually found in the wild-type protein at the position of Tyr73 (Table 6).

One of the reasons for this mutational study was to examine whether the aromatic ring was the only feature responsible for maintaining the histidine plane orientation (*18*, *19*). This, as is clear, is not the case; His77 has exactly the same orientation with respect to the heme plane as it does in the wild-type protein structure (rmsd = 0.18 Å). Probably, it is the hydrogen bond to the main chain C=O group of residue 73 (distance His77 N$\epsilon$2−Glu73 O of 2.8 Å), still present in the mutant structure, which is responsible for keeping the histidine plane in place.

The overall rearrangement of the charged residues around the solvent-exposed heme 4 edge has influenced one of the heme propionate groups of heme 2 (Table 5). The most striking change, as mentioned above, is the conformational change of Arg74, which forms a different salt bridge with heme 2 propionate A. This gives rise to a different hydrogen bonding environment for this propionate group, since the N$\eta$1 of Arg74 is now connected with Thr67 O (3.01 Å), a hydrogen bond which does not exist in the wild-type protein. Besides this evident change, small changes are observed for the heme propionate groups of hemes 3 and 4. It seems that the bonding of propionate A of heme 4 is weaker in the mutant structure than in the wild-type structure, since all hydrogen bonds are a little longer (Table 5), however, within the limits of error. The responsible residues, Lys22 and Lys23, have surely changed conformation though, and this could explain the elongation of the hydrogen bonds with this propionate group.

All together, the structural changes observed are concentrated around hemes 2 and 4. The most important impact is expected for heme 4, which is closest to Tyr73. On the other hand, no repercussion of the mutation was observed in the heme 1 vicinity, from a structural point of view. This heme is thus expected to be the least affected with respect to functional properties.

## DISCUSSION

*Effect of the Mutation on Structural Features.* Conserved residues are generally thought to have either a structural or functional importance, or both. We have analyzed the effect of the replacement of a highly conserved residue in the dimeric octaheme cytochrome $c_3$ from DdN, namely Tyr73, which was replaced by a glutamate residue. The mutant cytochrome is indistinguishable from the wild-type protein with respect to several biophysical and biochemical properties (*14*). The overall structural fold as well as the crystal packing has not changed with the mutation. Tyrosine 73 is an aromatic, not very polar residue located near heme 4, and in particular, its ring plane is parallel to the pyrrole ring of histidine 77, the sixth axial ligand of heme 4. The mutation was therefore expected to have an influence on the redox potential, and consequently on the intermolecular electron-transfer reaction, and/or the interaction with the physiological partner. Moreover, Tyr73 was thought to be responsible for the orientation of the histidine plane. However, the heme 4 axial ligands are still almost parallel to each other in the mutant cytochrome; therefore, His77 did not make a conformational change. The side chain of Tyr73 is not involved in the relative orientation of the axial ligands of the heme 4 iron atom. Other structural features, such as the hydrogen bond between the carbonyl group of the residue 73 and histidine 77 N$\epsilon$2, which is present in both wild-type and mutant cytochromes, seem to be important for maintaining the histidine plane orientation. It is noteworthy that the Y73E substitution does induce an important change in the histidine

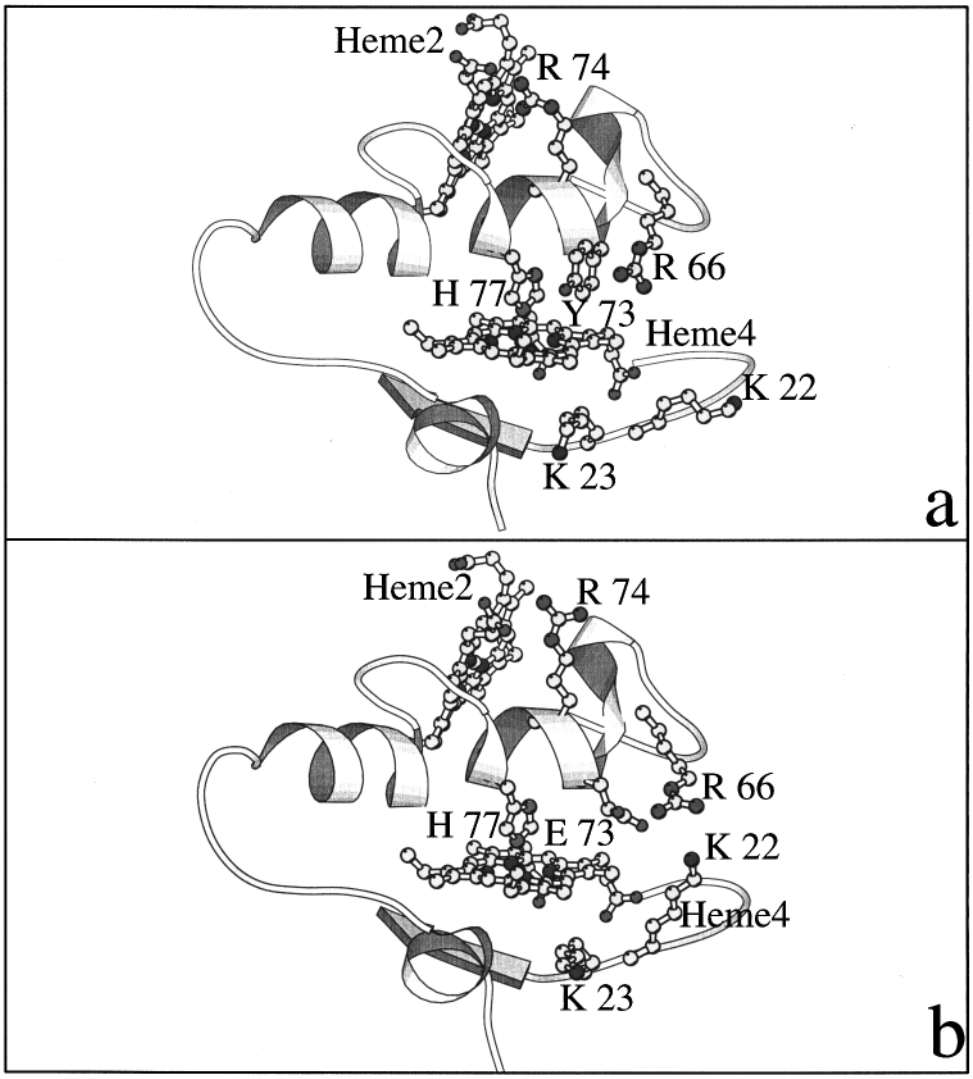


FIGURE 6: Schematic drawing of the structural model obtained after refinement in the region containing the mutation. The orientations are the same as those underlying the surface calculations represented in Figure 5. (a) The wild-type octaheme cytochrome $c_3$. (b) The Y73E octaheme cytochrome $c_3$. The conformational changes of residues Lys22, Arg66, and Arg74, induced by the mutation of tyrosine 73 into a glutamate, are clearly visible. The illustration was produced with MOLSCRIPT (*48*).

77 environment. But this change concerns the solvent exposure of this histidine, which is increased so that it becomes almost identical with that observed in the tetraheme cytochrome $c_3$ from DdN. This possibly has an influence on the redox potential of this heme group.

*Impact of the Point Mutation on the Redox Potentials*. As has been shown for monoheme cytochromes *c*, the most important factors on heme potential regulation are features such as the hydrophobicity of the heme pocket or the solvent exposure of the heme groups and especially the propionate groups (*12*). It is however difficult to make a direct correlation between monoheme and multiheme cytochromes, since the redox potentials of the different heme groups in multiheme cytochromes are often highly correlated and changes in the vicinity of one heme also influence the potentials of the other heme groups. In our case, this clearly is what has happened. A residue on the outward edge of the protein, in the vicinity of heme 4, has induced a global shift of the four redox potentials. The potentials have not yet been assigned to particular heme groups for this protein, but the observed values of −215, −280, −320, and 365 mV in the case of the wild-type cytochrome and −175, −220, −260, and −335 mV (*14*) in the case of the mutant protein are in agreement with minor structural changes around the heme groups. Since a hydrophobic, only slightly polar residue, tyrosine, has been replaced by a charged residue in the heme pocket of heme 4, one expects a drastic change in the potential of this heme group. The measured shifts of the macroscopic potentials, however, can only be explained by changes occurring for two of the heme groups or a strong correlation between the potentials or a combination of both. Looking at the structural changes introduced with the mutation, it appears that for at least two of the heme groups the features, which are supposed to be important for the heme potential modulation, have been perturbed; for heme 4, the polarity of the heme pocket is increased, as is the solvent exposure of the heme and one of the axial ligands, His77. It is therefore evident that the potential of this heme has changed. The same is true for heme 2. The heme environment has changed due to the conformational twist of Arg74; the propionate coordination, which is an important factor for potential modulation (*37*), has been perturbed, and the solvent exposure of the heme edge has significantly decreased. In the former case, a decrease of the potential is expected, while

Table 4: Overall Root-Mean-Square Deviations (Å) and Some Selected Residues and Their Implication in Salt Bridges or Hydrogen Bonds (Å)

| atom group/residue | rmsd | contacted residue | closest distance |
|---|---|---|---|
| all protein atoms | 1.20 | – | – |
| main chain atoms | 0.59 | – | – |
| side chain atoms | 1.26 | – | – |
| all heme atoms | 0.41 | – | – |
| heme 2 atoms | 0.81 | – | – |
| heme 1, 3, and 4 atoms | 0.23/0.30/0.29 main chain/ side chain | – | – |
| Lys22 | 0.42/3.41 | Glu73 | 4.02 |
| Lys23 | 0.25/0.79 | – | – |
| Lys64 | 0.43/2.07 | – | – |
| Glu65 | 0.33/2.11 | Asn62 | 2.93 |
| Arg66 | 0.24/2.30 | Glu73 | 3.19 |
| Glu68 | 0.24/2.10 | – | |
| Arg74 | 0.15/1.67 | heme 2 propionate | 2.94 |
| | | Thr67 | 3.01 |
| Lys80 | 0.48/1.39 | – | – |
| Asp100 | 0.24/1.54 | – | – |
| Gln111 | 3.69/8.21 | Arg66(sym) | 3.84 |
| | | Asn106 | 3.41 |

Table 5: Heme Propionate Coordination in Wild-Type and Y73E Octaheme Cytochromes $c_3$[a]

| heme atom | | atom in close contact in wild-type cytochrome | | atom in close contact in mutant cytochrome | |
|---|---|---|---|---|---|
| heme 1 | O1A | S53 N | 3.70 | S53 N | 3.57 |
| | | – | – | $O_w$ 245 | 2.86 |
| | O2A | – | – | – | – |
| | O1D | S53 O$\gamma$ | 2.73 | S53 O$\gamma$ | 2.68 |
| | | C54 N | 2.95 | C54 N | 2.91 |
| | O2D | S53 O$\gamma$ | 3.80 | S53 O$\gamma$ | 3.69 |
| | | – | – | $O_w$ 245 | 2.75 |
| | | – | – | $O_w$ 241 | 2.70 |
| heme 2 | O1A | R74 N$\eta$1 | 3.09 | R74 N$\epsilon$ | 2.94 |
| | | R74 N$\eta$2 | 2.94 | R74 N$\eta$2 | 2.97 |
| | O2A | – | – | $O_w$ 272 | 2.71 |
| | | – | – | $O_w$ 298 | 3.30 |
| | O1D | $O_w$ 249 | 3.43 | $O_w$ 297 | 2.76 |
| | | – | – | $O_w$ 298 | 2.87 |
| | O2D | $O_w$ 249 | 3.32 | $O_w$ 297 | 3.47 |
| | | $O_w$ 245 | 3.15 | $O_w$ 286 | 2.79 |
| heme 3 | O1A | N29 N$\delta$2 | 3.44 | N29 N$\delta$2 | 3.55 |
| | | S32 O$\gamma$ | 2.61 | S32 O$\gamma$ | 2.74 |
| | | $O_w$ 201 | 2.92 | $O_w$ 207 | 2.75 |
| | O2A | N29 N$\delta$2 | 3.43 | N29 N$\delta$2 | 3.86 |
| | | $O_w$ 201 | 2.98 | $O_w$ 207 | 3.67 |
| | O1D | $O_w$ 227 | 3.14 | $O_w$ 238 | 3.08 |
| | O2D | $O_w$ 227 | 2.92 | – | – |
| heme 4 | O1A | K22 N | 3.22 | K22 N | 3.48 |
| | | K23 N | 2.91 | K23 N | 2.93 |
| | | $O_w$ 216 | 2.81 | $O_w$ 209 | 2.65 |
| | O2A | Y10 O$\eta$ | 2.85 | Y10 O$\eta$ | 2.71 |
| | | K22 N | 2.89 | K22 N | 2.88 |
| | | K23 N | 3.40 | K23 N | 3.87 |
| | O1D | $O_w$ 216 | 2.80 | $O_w$ 209 | 2.78 |
| | O2D | P13 N | 3.48 | P13 N | 3.60 |
| | | $O_w$ 216 | 3.30 | $O_w$ 209 | 3.68 |

[a] The distances are in angstroms.

an increase of the potential is expected in the latter. For the two other heme groups, 1 and 3, no drastic structural changes are observed. Shifts of the potentials for these heme groups can only be explained by the cooperativity of the four-heme arrangement.

Table 6: Solvent Exposure (Å$^2$) of the Heme Groups and Axial Ligands in Wild-Type and Mutant Octaheme Cytochrome $c_3$ as Compared to That in Tetraheme Cytochrome $c_3$ from DdN[a]

| group of cytochrome $c_3$ | solvent exposure | | group of tetraheme cytochrome $c_3$ from DdN | solvent exposure |
|---|---|---|---|---|
| | wild-type | mutant | | |
| heme 1 | 58 | 66 | heme 1 | 124 |
| heme 2 | 208 | 181 | heme 2 | 323 |
| heme 3 | 184 | 182 | heme 3 | 203 |
| heme 4 | 78 | 94 | heme 4 | 95 |
| His30 | 2 | 0 | His36 | 9 |
| His33 | 0 | 0 | His39 | 1 |
| His42 | 0 | 0 | His48 | 0 |
| His43 | 33 | 25 | His49 | 75 |
| His60 | 0 | 0 | His67 | 1 |
| His77 | 15 | 32 | His89 | 27 |
| His90 | 0 | 0 | His96 | 0 |
| His109 | 3 | 0 | His115 | 0 |
| Cys54 | 0 | 0 | Cys61 | 0 |
| Cys59 | 9 | 5 | Cys66 | 6 |
| Cys105 | 37 | 30 | Cys111 | 41 |
| Cys108 | 1 | 0 | Cys114 | 2 |

[a] Calculated with TURBO-FRODO (*38*); $H_2O$ radius of 1.4 Å.

*Consequences of the Mutation on the Interaction with the Physiological Partner, the [NiFeSe] Hydrogenase.* The only interaction studies between cytochrome $c_3$ and the physiological partner, the hydrogenase, that have been published up to date are the measurement of the second-order rate constant by electrochemical methods (*39*). Preliminary results on the interaction of octaheme cytochrome $c_3$ and hydrogenase have been published recently (*14*). To compare the interaction properties of the mutant cytochrome with those of the wild-type cytochrome, the BIAcore measurements were carried out under the same conditions for both cytochromes. The apparent dissociation constant of the complex between oxidized hydrogenase and oxidized wild-type octaheme cytochrome $c_3$ was found to be $3.6 \times 10^{-6}$ M, which is on the same order of magnitude as those for other electron-transfer complexes (*40*, *41*). In the case of the oxidized Y73E mutant cytochrome, no interaction was detected even at high cytochrome concentrations, suggesting that this apparent dissociation constant must be higher than $10^{-3}-10^{-4}$ M. Therefore, the most important consequence of the mutation is the drastic change in the interaction of the mutant cytochrome with the [NiFeSe] hydrogenase. This result is also confirmed by the kinetic measurements at the steady state, where a $K_m$ value 14 times higher than that of the wild-type was found for the mutant cytochrome. These experiments, which are performed for the physiological partners in different oxidation states, favor the complex formation and make it possible to measure a $K_m$ value in the case of the mutant protein. The $K_m$ value of the interaction of the wild-type cytochrome with [NiFeSe] hydrogenase obtained here is similar to $K_m$ values reported for the interaction of the [NiFe] hydrogenase with the tetraheme cytochrome $c_3$ of Dg (*42*) and for the [Fe] hydrogenase with cytochromes from the same bacterial strain DvH (*35*). However, the kinetic measurements at the steady state of cytochrome reduction by the hydrogenase clearly show that the electron transfer between the physiological partners still takes place, since the $k_{cat}$ values are on the same order of magnitude for both wild-type and mutant proteins. These values are about 50 times lower than those reported by Verhagen et al. (*35*), but this is due to the lack of catalytic

efficiency of the [NiFeSe] hydrogenase in the hydrogen consumption reaction, compared to the [Fe] hydrogenase. Therefore, the point mutation has a drastic effect on the complex formation but not on the electron transfer itself. This observation can be related to other examples analyzing the role of aromatic residues on the interface between physiological partners of electron-transfer complexes. Analysis of several mutants of Phe82 in the yeast iso-1-cytochrome *c* has emphasized the role of this residue in maintaining the integrity of the interactive surface of the molecule, rather than as a direct intermediate in the intermolecular electron exchange (*43*). In the same way, replacement of the tyrosine 182 in the L subunit of the photosynthetic reaction center from *Rhodopseudomonas viridis* led to the conclusion that this aromatic residue was not required for the fast electron transfer from the heme $c_{559}$ of the cytochrome subunit to the special pair of bacteriochlorophylls. However, it was suggested that this residue might have a function in mediating an ideal docking of the cytochrome subunit with the L and M subunits (*44*). The structural analysis of the environment of heme 4 and its heme edge, which would be the surface of interaction with the physiological partner, shows that the lack of complex formation can be explained by the conformational changes occurring for the two positivly charged residues Lys22 and Arg66. If these residues are important for the docking with the physiological partner, their efficiency is drastically reduced in the case of the mutant protein, since they are turned parallel to the protein surface and are furthermore implicated in hydrogen bonding (Lys22) and in the formation of a salt bridge (Arg66) with the residue introduced by the mutation, while they are pointing into the solvent region in the wild-type protein structure. These residues have already been described to be possibly involved in the interaction with a physiological partner. The structural superposition (*10*) with the other representatives of the $c_3$ family implies that they correspond to lysine and arginine residues, which have been shown to be important for the interaction with physiological partners (*45*, *46*). Once the complex is formed, the electron-transfer reaction occurs with the same efficiency as in the complex involving the wild-type cytochrome. Thus, the energetic barrier for the complex formation between the hydrogenase and mutant cytochrome is higher than that involving the wild-type cytochrome. This analysis is in agreement with previous results on monoheme cytochrome *c*, showing that the complex most stabilized by electrostatic interactions is not imperatively the most efficient for the intermolecular electron-transfer reaction (*41*). Furthermore, it should be related to the Koshland's induced fit theory (*47*). To have a better understanding of the complex formation between these two physiological partners, it would therefore be interesting to analyze the properties of other mutants of Tyr73, but not to replace this residue with a charged one, or to analyze mutants of Lys22 and Arg66 with respect to protein−protein interaction with physiological partners. The crystal structure of the octaheme cytochrome $c_3$−hydrogenase complex would also give a solid foundation for a better comprehension of the electron-transfer complex between these two physiological partners.

## REFERENCES


1. Poulos, T. L., and Kraut, J. (1980) *J. Biol. Chem. 255*, 10322−10330.
2. Pelletier, H., and Kraut, J. (1992) *Science 258*, 1748−1755.
3. Hazzard, J. T., Mauk, A. G., and Tollin, G. (1992) *Arch. Biochem. Biophys. 298*, 91−95.
4. Mauk, G. A. (1991) *Struct. Bonding (Berlin) 75*, 131−157.
5. Couthino, I. B., and Xavier, A. V. (1994) *Methods Enzymol. 243*, 119−140.
6. Bruschi, M. (1994) *Methods Enzymol. 243*, 140−155.
7. Pollock, W. B. R., Loutfi, M., Bruschi, M., Rapp-Giles, B. J., Wall, J. D., and Voordouw, G. (1991) *J. Bacteriol. 173*, 220−228.
8. Ambler, R. P. (1980) in *From cyclotrons to cytochromes* (Robinson, A. B., and Kaplan, N. O., Eds.) pp 263−279, Academic Press, London.
9. Czjzek, M., Payan, F., Guerlesquin, F., Bruschi, M., and Haser, R. (1994) *J. Mol. Biol. 243*, 653−667.
10. Czjzek, M., Guerlesquin, F., Bruschi, M., and Haser, R. (1996) *Structure 4*, 395−404.
11. Bruschi, M., Loutfi, M., Bianco, P., and Haladjian, J. (1984) *Biochem. Biophys. Res. Commun. 120*, 384−389.
12. Mathews, F. S. (1985) *Prog. Biophys. Biol. 45*, 1−56.
13. Voordouw, G., and Brenner, S. (1986) *Eur. J. Biochem. 159*, 347−351.
14. Aubert, C., Leroy, G., Bruschi, M., Wall, J. D., and Dolla, A. (1997) *J. Biol. Chem. 272*, 15128−15134.
15. Dolla, A., Florens, L., Bianco, P., Haladjian, J., Voordouw, G., Forest, E., Wall, J., Guerlesquin, F., and Bruschi, M. (1994) *J. Biol. Chem. 269*, 6340−6346.
16. Saraiva, L. M., Salguiero, C. A., LeGall, J., vanDongen, W. M. A. M., and Xavier, A. V. (1996) *JBIC, J. Biol. Inorg. Chem. 1*, 542−550.
17. Higuchi, Y., Kusunoki, M., Yasuoka, N., Kakudo, M., and Yagi, T. (1981) *J. Biochem. 90*, 1715−1723.
18. Czjzek, M., Payan, F., and Haser, R. (1994) *Biochimie 76*, 546−553.
19. Higuchi, Y., Kusunoki, M., Matsuura, Y., Yasuoka, N., and Kakudo, M. (1984) *J. Mol. Biol. 172*, 109−139.
20. Odom, J. M., and Peck, H. D., Jr. (1984) *Annu. Rev. Microbiol. 38*, 551−592.
21. Haladjian, J., Bianco, P., Guerlesquin, F., and Bruschi, M. (1990) *Biochem. Biophys. Res. Commun. 179*, 605−610.
22. Postgate, J. R. (1984) in *The sulfate reducing bacteria*, 2nd ed., pp 24−41, Cambridge University Press, Cambridge, U.K.
23. Marquardt, D. W. (1963) *J. Soc. Indust. Appl. Math. II*, 431−441.
24. Czjzek, M., Guerlesquin, F., Roig, V., Payan, F., Bruschi, M., and Haser, R. (1992) *J. Mol. Biol. 228*, 995−997.
25. Otwinowski, Z. (1993) in *Proceedings of the CCP4 Study Weekend: "Data Collection and Processing"* (Sawyer, L., Isaacs, N., and Bailey, S., Eds.) pp 56−62, SERC Daresbury Laboratory, Warrington, U.K.
26. Minor, W. (1993) *XDISPAYF*, Purdue University, West Lafayette, IN.
27. Navaza, J. (1994) *Acta Crystallogr. A 50*, 157−163.
28. Brünger, A. T. (1996) *X-PLOR*, Version 3.8, Yale University, New Haven, CT.
29. Ramachandran, G. N., and Sasisekharan, V. (1968) *Adv. Protein Chem. 23*, 283−437.
30. Luzzati, V. (1952) *Acta Crystallogr. 5*, 802−810.
31. Nicholls, A., Sharp, K. A., and Honig, B. (1991) *Proteins 11*, 281−296.
32. Nicholls, A., and Honig, B. (1991) *J. Comput. Chem. 12*, 435−445.
33. Schuck, P., and Minton, C. (1996) *Trends Biochem. Sci. 21*, 458−460.
34. Voordouw, G. (1992) in *The sulfate reducing bacteria: contemporary perspectives*, pp 88−130, Springer-Verlag, New York.
35. Verhagen, M. F. J. M., Wolbert, R. B. G., and Hagen, W. R. (1994) *Eur. J. Biochem. 221*, 821−829.
36. Stellwagen, E. (1978) *Nature 275*, 73−74.
37. Bertrand, P., Mbarki, O., Asso, M., Blanchard, L., Guerlesquin, F., and Tegoni, M. (1995) *Biochemistry 34*, 11071−11079.
38. Roussel, A., and Cambillau, C. (1992) *TURBO-FRODO, the*

*manual*, Biographics, AFMB, Marseille, France.
39. Haladjian, J., Bianco, P., Guerlesquin, F., and Bruschi, M. (1991) *Biochem. Biophys. Res. Commun. 179*, 605−610.
40. Guerlesquin, F., Sari, J. C., and Bruschi, M. (1987) *Biochemistry 26*, 7438−7443.
41. Hazzard, J. T., McLendon, G., Cusanovich, M. A., Das, G., Sherman, F., and Tollin, G. (1988) *Biochemistry 27*, 4445−4451.
42. Niviere, V., Hatchikian, E. C., Bianco, P., and Haladjian, J. (1988) *Biochim. Biophys. Acta 935*, 34−40.
43. Lo, T. P., Guillemette, J. G., Louie, G. V., Smith, M., and Brayer, G. D. (1995) *Biochemistry 34*, 163−171.
44. Dohse, B., Mathis, P., Wachtveitl, J., Laussermair, E., Iwata, S., Michel, H., and Oesterhelt, D. (1995) *Biochemistry 34*, 11335−11343.
45. Stewart, D. E., Legall, J., Moura, I., Moura, J. J. G., Peck, H. D., Xavier, A. V., Weiner, P. K., and Wampler, J. E. (1989) *Eur. J. Biochem. 185*, 695−700.
46. Dolla, A., Leroy, G., Guerlesquin, F., and Bruschi, M. (1991) *Biochim. Biophys. Acta 1058*, 171−177.
47. Koshland, D. E., Jr. (1958) *Proc. Natl. Sci. Acad. U.S.A. 44*, 98−104.
48. Kraulis, P. J. (1991) *J. Appl. Crystallogr. 24*, 946−950.

BI971656G